



Research Paper

Validation of the Critical Buckling Load of A Single-Layer Laminated Composite Nanoplate Under Various Boundary Conditions

R VITTAL¹, CHANDRAPPA S², ANANDA C B³

¹ Senior Scale Lecturer, Department of Mechanical Engineering, Government polytechnic Mulabagal, Karnataka, India.

² Lecturer, Department of Mechanical Engineering, Government polytechnic K.G.F, Karnataka, India.

³ Senior Scale Lecturer, Department of Mechanical Engineering, Government polytechnic Channasandra, Karnataka, India.

Abstract

The buckling behavior of single-layer armature-type graphene nanoplates of various sizes is examined in this work in relation to the impact of atomic vacancy defects with variable distributions. This study is novel because it thoroughly examines the effects of elements that have received little attention in previous research, including aspect ratio, defect concentration, clamped-free (CF), clamped-clamped (CC), and simply-supported (SS) boundary conditions, on the buckling behavior of graphene nanoplates. To maintain the discrete character of the nanoplates, a novel technique was used to describe them using space frame structures. The buckling behavior was predicted using the finite element method (FEM). Through comparison with pertinent data published in the open literature, the simulation findings for the critical buckling load (P_{cr}) were verified. According to the results, P_{cr} dramatically drops at low aspect ratios when this factor is reduced, although this decline becomes more gradual at larger aspect ratios. Furthermore, it was shown that atomic-scale flaws significantly decreased P_{cr} ; for example, a 10% concentration of defects resulted in a roughly 40% decrease in the critical buckling load, underscoring the important role that defects play in the stability of nanostructures.

Keywords: Graphene nanoplate; Layers; Buckling load; Defects.

I. INTRODUCTION AND LITERATURE REVIEW

Growing interest has been sparked by recent developments in the research of nanoplates, which have two-dimensional nanoscale structures. Because of its exceptional qualities and wide variety of possible uses, single-layer and multilayer graphene sheets are among the most studied nanoplates [1,2]. Because of its exceptional mechanical, electrical, and thermal properties, graphene—the strongest and thinnest substance known—has gained attention. Graphene nanoplates' special qualities make them attractive options for a wide range of uses in industries including biomedical technologies [8], solar energy systems [7], transistors [6], electromechanical devices [3], nanosensors [4], and nanoactuators [5]. These materials have the potential to revolutionize the electronics, energy storage, and healthcare sectors, which is why there is a great deal of theoretical and experimental study being done to examine how they behave under different operating situations. The finite element method (FEM) and computational techniques from the viewpoints of atomic, continuum, and molecular mechanics are used in the first set of theoretical investigations. Although each of these approaches has pros and cons, several researchers have used them to look at various facets of nanostructures, especially graphene. The mechanical behavior of single-layer graphene sheets has been accurately and consistently analyzed using atomic-based techniques such density functional theory, tight-binding, and molecular dynamics (MD) [9]. The mechanical behavior of graphene sheets, including ultimate strength, Young's modulus, and variations in Young's modulus and shear modulus at various temperatures, has been examined by several researchers using molecular dynamics simulations. Wang and Zhang recently computed the Young's modulus and fracture toughness of bilayer graphene using MD simulations, demonstrating that although temperature has little influence on the elastic modulus, it is a major factor in fracture toughness [10]. In a different research, Wang et al. looked at the failure of imperfect graphene that had vacancies and Stone-Wales (S-W) defects. [11]. Using MD simulations, Fadaei Heydari et al. [12] investigated how graphene oxide nanoparticles (GO-NP)

affected the mechanical and thermal characteristics of PU/PCL nanocomposites. They discovered that the optimal balance was achieved at a 2% GO-NP concentration, which improved mechanical strength, heat flux, and thermal conductivity without degrading the material's qualities.

The continuum-based technique, which successfully simulates the unique characteristics of small-scale structures, is the foundation of the second theoretical approach. This technique was used by Behfar and Naghdabadi to investigate the vibration properties of multilayer graphene sheets immersed in an elastic media [13]. An analytical method for predicting the flexural modulus of multilayer graphene sheets was also presented in another paper [14]. A continuum-plate model was created by Kitipornchai et al. [15] to analyze the vibrations of multilayer graphene sheets.

Using both classical and non-classical theories, such as the implicit gradient, non-local differential form, first-order strain gradient, and second-order strain gradient, Jafari et al. [16] investigated the free vibration behavior of nanoplates. They evaluated the effects of characteristics including classical and nonlocal properties, boundary conditions, and plate dimensions while numerically solving partial differential equations and determining parametric responses for natural frequencies using the Navier and Galerkin approaches. Furthermore, Namin and Pilafkan [17] examined the vibrational behavior of defective graphene sheets using nonlocal elasticity theory, showing that atomic structural defects lower the natural frequencies of these sheets.

The scaling constraints of atomic and continuum-based simulations have given rise to a third theoretical viewpoint and the creation of multiscale computing techniques. By combining molecular mechanics and finite element methods (FEM), these techniques provide atomic-scale FEM models that accurately represent force fields, atomic interactions, and nanoscale phenomena without the need for standard FEM approximations. Compared to molecular dynamics simulations, this method lowers computing costs while enabling the evaluation of carbon nanostructures' buckling force, natural frequencies, and vibration modes [18, 19].

The atomic finite element technique (AFEM) was first presented by Liu et al. [20], and its use was subsequently expanded to examine the mechanical behavior of single-walled carbon nanotubes [21]. Gu et al. plotted their strain energy curves using AFEM to examine local buckling in bent single-walled carbon nanotube models [22]. Similarly, Pradhan [23] investigated how nanoscale factors affected single-layer graphene's critical buckling stress and found that buckling ratios rose with nonlocal parameter values and fell with graphene sheet length. In order to describe single-layer graphene sheets and evaluate its buckling behavior in an elastic media, Samaei et al. [24] used nonlocal Mindlin plate theory. Zhang et al. [25] examined single-layer graphene sheet buckling in elastic environments using the element-free Kp-Ritz technique and non-local elasticity theory, highlighting the impact of surrounding elastic support and nonlocal factors on critical buckling patterns. In the meanwhile, Sakhaee-Pour [26] used molecular structural mechanics to analyze elastic buckling and discovered a nonlinear connection between buckling force and sheet width, with no discernible impact from aspect ratio.

II. FEM SIMULATIONS

The numerical simulations are carried out using a mix of ANSYS and MATLAB. To do this, the necessary MATLAB algorithms were created to build the model geometry, and the data was then imported into ANSYS to carry out the solution and apply boundary conditions. Additionally, a MATLAB script was created to produce a command code that is then run in ANSYS. As shown in Fig. 1, the model depicts a two-dimensional structure with length a and breadth b , as well as the coordinate system that is being used. The first step in the modeling technique is to define points that represent carbon atoms. These points are then connected by lines that represent covalent bonds. A single unit cell is created and duplicated along the x - and y -axes to create the planar structure, creating a full two-dimensional lattice.

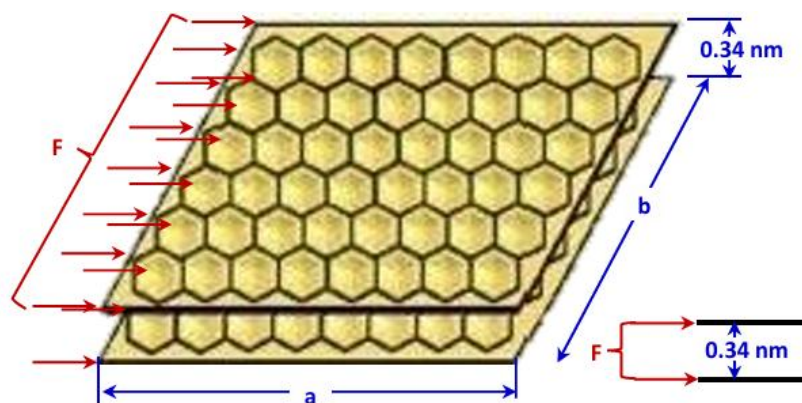


Fig. 1. Interlayer distance in double-layer graphene nanoplates under compression load causing buckling.

The three-dimensional BEAM4 elastic element was used to describe the covalent bonds within the graphene structure. Three translational degrees of freedom along the x , y , and z axes and three rotational degrees of freedom around these axes are included in every node in this model. In order to depict van der Waals interactions between neighboring layers, interlayer springs were also included. Only when the interatomic distance was equal to or less than the cutoff radius, represented by σ (the Lennard-Jones parameter), were these interactions taken into account. Atoms were considered to have no interaction beyond this level. The stiffness values of the springs were determined using an equivalency method that connected the elastic energy of the springs to the chemical bond energy after they were specified between atomic sites.

A number of nanoplates with two width values of 30 Å and 70 Å and different lengths were examined in order to look at the buckling behavior. Actually, to enable the examination of the impact of the aspect ratio, a/b , nanoplates of varying length were created for each width. Furthermore, different vacancy concentrations were added to the nanoplate's shape in order to demonstrate how atomic defects affect its buckling ability. Since boundary conditions also have a significant impact on buckling behavior, the various kinds listed in Table 1 were included in the simulations. The letters CF, CC, and SS stand for clamped-free, clamped-clamped, and simply supported boundary conditions, respectively, for the sake of conciseness.

III. APPLIED BOUNDARY CONDITIONS

Table 1 Different applied boundary conditions in buckling analysis

Nanoplate face	Clamped-Free	Clamped-Clamped	Simply-Simply
$y = 0$	All DOF = 0	All DOF = 0	$u_x = 0; u_y = 0; u_z = 0$
$y = a$	$F_y = P$	$u_x = 0; u_z = 0; F_y = P$ All rotation = 0	$u_x = 0; u_z = 0; F_y = P$

IV. VALIDATION

A comparison was made between the findings of the suggested model for the buckling analysis of graphene nanoplates and the results of reference. This was done in order to verify the system. For the purpose of this validation, a flawless single-layer nanoplate measuring 201.68 Å in length (as shown in Figure 2) was examined for a number of different aspect ratios. The comparison, which is shown in Figure 2, demonstrates that there is considerable concordance with the reference data, which substantiates the correctness and dependability of the model that was built.

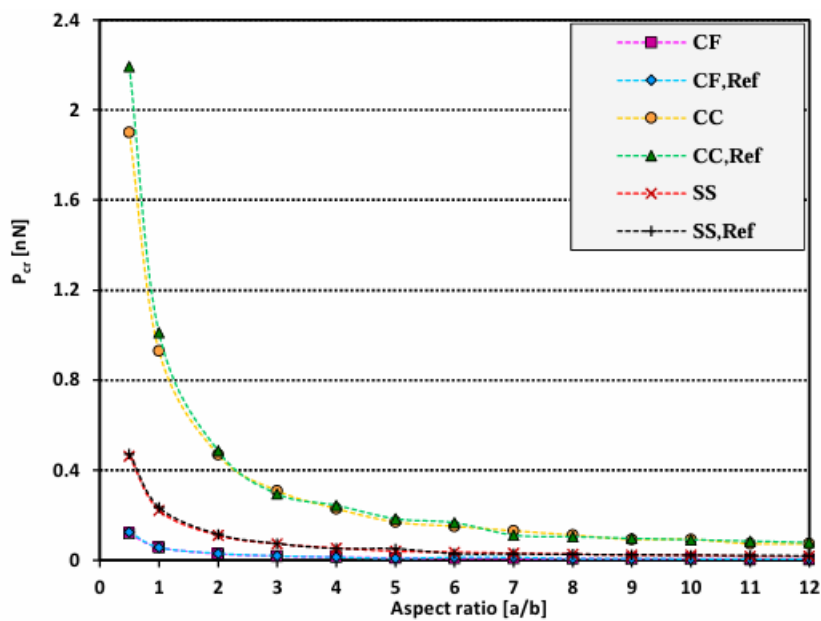


Fig. 2. Comparison and validation of the critical buckling load of a single-layer nanoplate with a length of 201.68 Å

V. RESULTS AND DISCUSSION

In this part, the results of the buckling analysis are presented for both single-layer and double-layer graphene nanoplates. The study takes into consideration the presence or absence of defects. The nanoplates, which have widths of 30 Å and 70 Å, and aspect ratios that vary, are subjected to three distinct boundary conditions, namely CF, CC, and SS, while a uniform compressive force (P) is applied at one end.

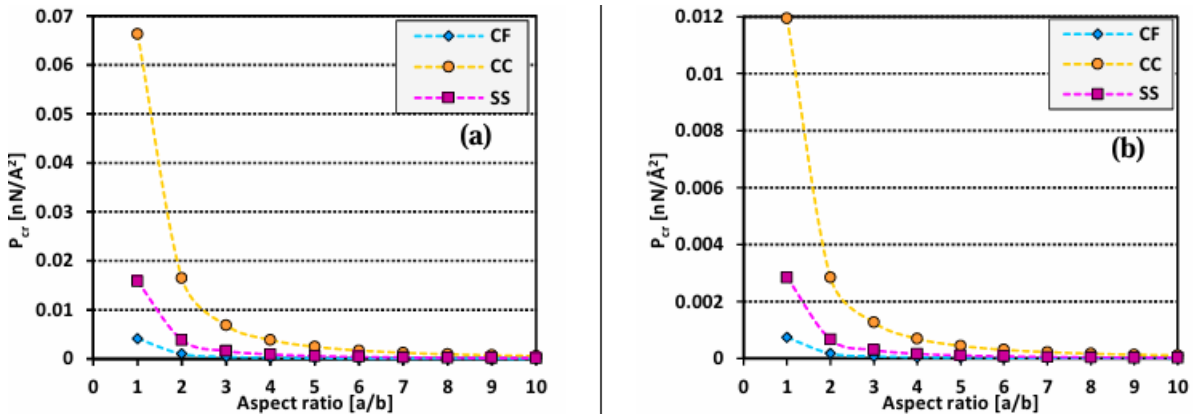


Fig. 3. Dependence of the critical buckling load (P_{cr}) for a perfect single-layer nanoplate as a function of aspect ratio, for nanoplates with widths: (a) 30 Å, and (b) 70 Å.

The graph in Figure 3 depicts the fluctuation of the critical buckling load per unit area (P_{cr}) for graphene nanoplates with widths of 30 Å and 70 Å in relation to the aspect ratio, a/b . According to the findings, the value of P_{cr} exhibits a substantial range of variation in a downward direction for all three border conditions when the aspect ratios are smaller. The rate of reduction in the buckling load, on the other hand, is slowed down when the aspect ratio is increased. The size-dependent mechanical characteristics of nanoplates at tiny length scales are responsible for this phenomenon, which will be discussed more below. In addition, the critical buckling load per unit area, denoted by the symbol P_{cr} , is presented for every nanoplate for the three distinct boundary conditions. Based on the findings, which are shown in Figure 4, it can be seen that the CC boundary condition exhibits the largest buckling load, followed by the SS and CF conditions. As the aspect ratio rises, the curves have a tendency to converge, as seen in the picture. Based on this, it seems that the effect of boundary conditions is reduced for bigger nanoplates, which is consistent with what was anticipated. By comparing the buckling loads of the two nanoplate sizes, it is evident that the buckling load for the nanoplate with a width of 30 Å is greater than the buckling load for the nanoplate with a width of 70 Å. Based on this, it may be deduced that nanoplates of a lower size demonstrate higher structural stability. This may be attributed to the fact that the vulnerability of the nanoplate to deformation and warping gets more severe as the width of the nanoplate grows.

VI. CONCLUSION

Using three distinct boundary conditions—clamped-free (CF), clamped-clamped (CC), and simply-simple (SS)—an investigation of the buckling behavior of single- and double-layer rectangular nanoplates was carried out. Moreover, the influence of the vacancy flaws was also investigated in another study. The following observations and results were derived from this investigation:

Based on the findings that were obtained, it was found that the width of the nanoplate, in addition to its length, has an effect on the buckling capacity per unit cross section area. This means that the buckling load is lower for a width of 70 Å than it is for a width of 30 Å. There is a possibility that this is related to the fact that the chance of local buckling rises as the sheet width grows, and as a result, the buckling load capacity of the graphene diminishes. At low values of the aspect ratio, the buckling load is said to have a significant dependence on the aspect ratio. However, as the aspect ratio grows, the reliance becomes less significant. This holds true for all three boundary conditions. When it comes to the boundary conditions, the buckling load that is produced by CC is the largest, followed by SS and CF. It has been noticed that the impact of the boundary conditions decreases as the size and aspect ratio of the object increases. As the size of the domain rises, the fraction of boundary edges compared to the overall domain decreases, which results in a lessened impact of boundary conditions. This is an essential point to underline from a physical point of view.

References

- [1]. H. Tong-Wei, H. Peng-Fei, W. Jian, W. Ai-hui, Molecular dynamics simulation of a single graphene sheet under tension, *New Carbon Mater.* 25 (2010) 261–266
- [2]. A. Nassar, E. Nassar, I. Rivilla, J. Labidi, A.G. Fernandez, F. Sarasini, Enhancing the thermal conductivity and shape stability of phase-change composites using diatomite and graphene nanoplates for thermal energy storage, *Results Eng.* 22 (2014) 102184.
- [3]. J.-S. Moon, D.K. Gaskill, Graphene: Its fundamentals to future applications, *IEEE Trans. Microw. Theory Tech.* 59 (2011) 2702–2708.
- [4]. Y. Xu, Z. Guo, H. Chen, Y. Yuan, J. Lou, X. Lin, H. Gao, H. Chen, B. Yu, In-plane and tunneling pressure sensors based on graphene/hexagonal boron nitride heterostructures, *Appl. Phys. Lett.* 99 (2011).
- [5]. G.W. Rogers, J.Z. Liu, Graphene actuators: quantum-mechanical and electrostatic double-layer effects, *J. Am. Chem. Soc.* 133 (2011) 10858–10863.
- [6]. M. Ryzhii, A. Satou, V. Ryzhii, T. Otsuji, High-frequency properties of a graphene nanoribbon field-effect transistor, *J. Appl. Phys.* 104 (2008).
- [7]. C.-T. Hsieh, B.-H. Yang, J.-Y. Lin, One-and two-dimensional carbon nanomaterials as counter electrodes for dye-sensitized solar cells, *Carbon N. Y.* 49 (2011) 3092–3097.
- [8]. L. Yang, L. Zhang, T.J. Webster, Carbon nanostructures for orthopedic medical applications, *Nanomedicine.* 6 (2011) 1231–1244.
- [9]. C. Li, T.-W. Chou, A structural mechanics approach for the analysis of carbon nanotubes, *Int. J. Solids Struct.* 40 (2003) 2487–2499.
- [10]. L. Wang, Q. Zhang, Elastic behavior of bilayer graphene under in-plane loadings, *Curr. Appl. Phys.* 12 (2012) 1173–1177.
- [11]. M.C. Wang, C. Yan, L. Ma, N. Hu, M.W. Chen, Effect of defects on fracture strength of graphene sheets, *Comput. Mater. Sci.* 54 (2012) 236–239.
- [12]. S.F. Heydari, M. Shahgholi, A. Karimipour, M. Salehi, S.A. Galehdari, The effects of graphene oxide nanoparticles on the mechanical and thermal properties of polyurethane/polycaprolactone nanocomposites; a molecular dynamics approach, *Results Eng.* 24 (2014) 102933.
- [13]. K. Behfar, R. Naghdabadi, Nanoscale vibrational analysis of a multi-layered graphene sheet embedded in an elastic medium, *Compos. Sci. Technol.* 65 (2005) 1159–1164.
- [14]. K. Behfar, P. Seifi, R. Naghdabadi, J. Ghanbari, An analytical approach to determination of bending modulus of a multi-layered graphene sheet, *Thin Solid Films.* 496 (2006) 475–480.
- [15]. S. Kitipornchai, X.Q. He, K.M. Liew, Continuum model for the vibration of multilayered graphene sheets, *Phys. Rev. B—Condensed Matter Mater. Phys.* 72 (2005) 75443.
- [16]. A. Jafari, S.S. Shah-enayati, A.A. Atai, Size dependency in vibration analysis of nano plates; one problem, different answers, *Eur. J. Mech.* 59 (2016) 124–139.
- [17]. S.F.A. Namin, R. Pilafkan, Vibration analysis of defective graphene sheets using nonlocal elasticity theory, *Phys. E Low-Dimensional Syst. Nanostructures.* 93 (2017) 257–264.
- [18]. B. Liu, Z. Zhang, Y. Chen, Atomistic Statics Approaches—Molecular Mechanics, Finite Element Method and Continuum Analysis, *J. Comput. Theor. Nanosci.* 5 (2008) 1891–1913.
- [19]. A. Alidoust, M. Haghgoo, R. Ansari, J. Jamali, M.K. Hassanzadeh-Aghdam, A numerical conductive network model for investigating the strain-sensing response of graphene nanoplatelets-filled elastomeric strain sensors, *Results Eng.* 24 (2014) 103341.
- [20]. B. Liu, Y. Huang, H. Jiang, S. Qu, K.C. Hwang, The atomic-scale finite element method, *Comput. Methods Appl. Mech. Eng.* 193 (2004) 1849–1864.
- [21]. B. Liu, H. Jiang, Y. Huang, S. Qu, M.-F. Yu, K.C. Hwang, Atomic-scale finite element method in multiscale computation with applications to carbon nanotubes, *Phys. Rev. B—Condensed Matter Mater. Phys.* 72 (2005) 35435.
- [22]. X. Guo, A.Y.T. Leung, X.Q. He, H. Jiang, Y. Huang, Bending buckling of single-walled carbon nanotubes by atomic-scale finite element, *Compos. Part B Eng.* 39 (2008) 202–208.
- [23]. S.C. Pradhan, Buckling of single layer graphene sheet based on nonlocal elasticity and higher order shear deformation theory, *Phys. Lett. A.* 373 (2009) 4182–4188.
- [24]. A.T. Samaei, S. Abbasion, M. Mirsayar, Buckling analysis of a single-layer graphene sheet embedded in an elastic medium based on nonlocal Mindlin plate theory, *Mech. Res. Commun.* 38 (2011) 481–485.
- [25]. Y. Zhang, L.W. Zhang, K.M. Liew, J. Yu, Buckling analysis of graphene sheets embedded in an elastic medium based on the kp-Ritz method and non-local elasticity theory, *Eng. Anal. Bound. Elem.* 70 (2016) 31–39.
- [26]. A. Sakhaee-Pour, Elastic buckling of single-layered graphene sheet, *Comput. Mater. Sci.* 45 (2009) 266–270.